C. R. Physique 15 (2014) 662–673

Contents lists available at ScienceDirect

Comptes Rendus Physique

www.sciencedirect.com

Liquid and solid foams / Mousses liquides et solides

Processing and structures of solids foams

Elaboration et structure des mousses solides

Luc Salvo [a,*], Guilhem Martin [a], Mathieu Suard [a], Ariane Marmottant [b], Rémy Dendievel [a], Jean-Jacques Blandin [a]

[a] *Grenoble University & CNRS, SIMaP/GPM2, UMR 5266, 101, rue de la Physique, BP 46, 38402 Saint-Martin-d'Hères cedex, France*
[b] *Constellium Technology Center, Parc économique Centr'alp, CS10027, 38341 Voreppe cedex, France*

ARTICLE INFO

Article history:
Available online 14 November 2014

Keywords:
Polymer
Ceramic
Metal
Foam
Processing
Structure

Mots-clés :
Polymère
Céramique
Métal
Mousse
Elaboration
Structure

ABSTRACT

This paper aims at presenting the main processing routes that are used to produce foams in their general definition and the typical structure that can be obtained according to the process. We first describe the main classification of the foam according to the level of porosity (open cells, closed cells, partially open cells and mixed cells). We present briefly the main processes to obtain such structures (non-removable space holder stacking and impregnation, removable space holder, foaming from gas or from precursor and shortly additive manufacturing) with a specific focus on the metal foam processing. We finally indicate the main structure that can be obtained with these types of processes and the main characteristics that are necessary to quantify at the various scale of the structure.

RÉSUMÉ

L'objectif de cet article est de présenter les principales voies de synthèse des mousses dans leur définition générale et la structure typique qui peut être obtenue en fonction de chacune d'entre elles. Nous décrivons d'abord la classification principale de la mousse selon son niveau de porosité (cellules ouvertes, fermées, partiellement ouvertes et mixtes). Nous présentons brièvement les principaux procédés permettant d'obtenir de telles structures (imprégnation ou empilement de particules poreuses, élimination de particules, bullage par injection de gaz ou à partir d'un précurseur et fabrication additive), en mettant plus spécifiquement l'accent sur la réalisation de mousses métalliques. Nous indiquons finalement la structure principale qui peut être obtenue par ces types de procédés et les caractéristiques principales qu'il est nécessaire de quantifier aux différentes échelles de la structure.

* Corresponding author.

http://dx.doi.org/10.1016/j.crhy.2014.10.006
1631-0705/

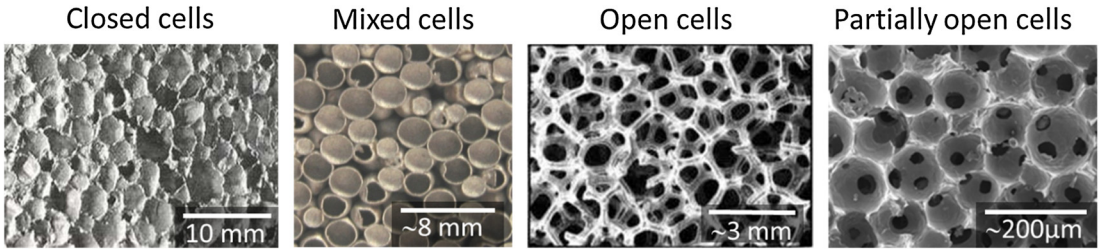

Fig. 1. The different kinds of cellular solids: from closed cells to open cells.

1. Introduction

According to Gibson and Ashby [1], a cellular solid is "one made up of an interconnected network of solid struts or plates which form edges and faces of cells". There are two types of cellular solids: (i) 2D cellular solids like "honeycombs", with a geometry that is defined in 2D, (ii) 3D cellular solids, which we will for simplicity call foams, present generally highly porous 3D structures that are divided into distinct cells, a cell being an empty space delimited by solid boundaries. Ideally, the individual cells are all separated from each other by material, but often this restriction is relaxed. In the latter category, one can distinguish between two subgroups: if the material is distributed in the faces and the struts of the cells, the cellular solid is often called closed-cell foams (syntactic foams can be classified in this category). If it is in the struts only (so that the cells connect through open faces), it is called open-cell foams. Intermediate configurations do exist (for example, cell faces are partly solid, or some faces are solid and others are open: in this case, we can use the term "partially open-cell foams". The last configuration is when the material presents at the same time open porosity and closed porosity like hollow-sphere stacking: we will call them mixed-cell foams. Fig. 1 presents the structure of all these foams. These definitions are valid whatever the constitutive material of the cellular structure: polymer, ceramic or metallic. Note that the term foam should be restricted to cellular materials that are produced by a foaming technique, which is often not the case for open-cell foams, partially open-cell foams and mixed-cell foams, as we will see. However, this term presents the advantage of simplicity and we will keep it to describe 3D cellular structures. The aim of the processing section is to give the general trends, highlighting some specificity according to the constitutive material, rather than presenting an exhaustive review of the processing of all the foams. The structure and the main parameters to characterize cellular solids are quite common to all cellular materials and thus the structural parameters will be presented in reference to foam characteristics (open, closed, partially open and mixed).

2. Processing

Fig. 2 presents the main processing routes that are used to process polymer, ceramic or metal porous materials. This section will be devoted to processes that allow obtaining highly porous materials, i.e. with a relative density larger than 60%. We will briefly present these processes and highlight some features according to the constitutive material: we will consider non-removable space holder stacking, non-removable space holder impregnation, removable space holder, foaming from gas or from precursor and finally additive manufacturing. We will not present in this paper sintered entangled materials.

2.1. Non-removable space holder stacking

The principle is to stack and join hollow particles in order to produce a 3D material. In order to get a structure than can hold, contacts have to be created permanently between the hollow objects. One example of this technique is the hollow metallic sphere stacking process that has been extensively studied over the last ten years [2]. The metallic hollow spheres can be produced from a polystyrene sphere on which metallic particles are deposited using suspension. So far, various materials such as iron, stainless steel, titanium and molybdenum have been used. A de-binding step is required to get rid of polystyrene, followed by a sintering stage to obtain a porous or dense shell. The metallic spheres are stacked (randomly or periodically) and sintered or glued together in order to get a 3D structure. The particularity of this structure is that it is possible to obtain a fully closed cell structure (with a tetrakaidecahedron unit cell) as well as a mixed cell structure with closed porosity (inside the sphere) and open porosity (between the spheres). The size of the spheres is typically a few millimeters, the shell thickness between 50 and 200 µm, and the typical relative density reached is between 0.1 and 0.3. The most developed material with this type of arrangement is stainless steel, but other types of metal can be used [2–4]. Aluminum foam granules [5] that are bonded together can also be used to produce a mixed-cell structure. This process develops under the trade mark APM uses aluminum foam granules of few millimeters in diameter with a relative density between 0.2 and 0.3, which are bonded and mixed, leading to a final product with a relative density as low as 0.1. Recently these granules have been used in polymer matrices as space holders in order to produce aluminum hybrid foam sandwiches as innovative materials for battery housings of electrical vehicles [6].

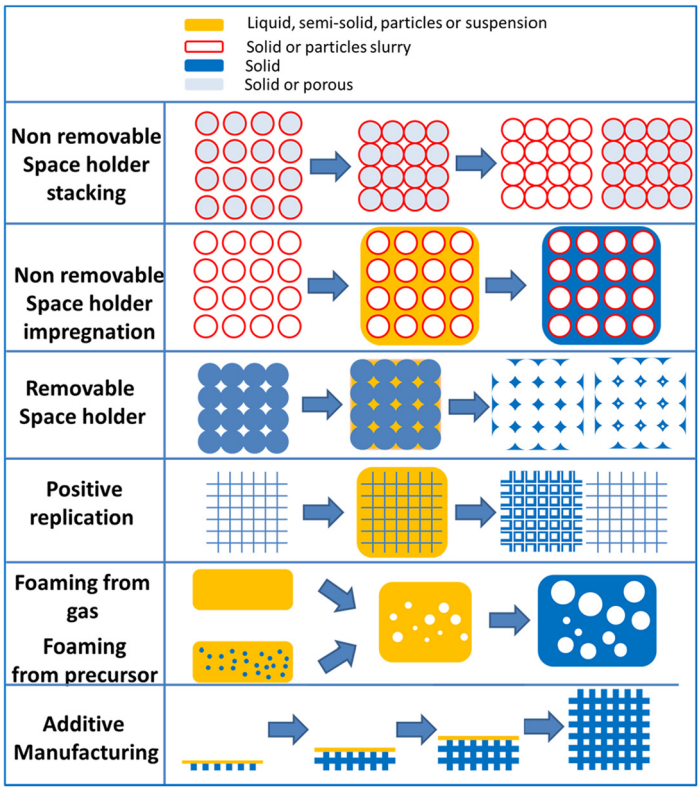

Fig. 2. (Color online.) The various processing routes of foams or porous structures.

2.2. Non-removable space holder infiltration

This technique is based on the use of micro-balloons or hollow sphere that are infiltrated or mixed with a metal, polymer or ceramic suspension. This is often called syntactic foams. The specificity of syntactic foams is to use a hollow sphere usually made of glass [7], but other types of hollow sphere exist, such as polymer, ceramic or even metallic ones [8–10]. These glass hollow spheres have been widely used in polymer matrices [11]. The diameter of these glass spheres is between 15 and 60 µm and the shell thickness is between 0.5 to 2 µm and their typical density between 0.1 and 0.6 g/cm^3. The crushing pressure is of course mainly influenced by the density and can vary between a few MPa and 200 MPa [8]. The use of the syntactic spheres requires care during processing in order not to crush the spheres and therefore a specific design of the screw for injection molding of syntactic polymer foams [7]. Ceramic hollow spheres have been used for example in aluminum metal matrices. A preform of the hollow sphere is infiltrated with aluminum using a low gas pressure and dedicated devices [12,13].

2.3. Removable space holder

This method has been extensively used for metallic foams. There are two main ways to produce foams with this technique: a powder metallurgy route and a casting route. In the powder metallurgy route the removable space holder, usually polymer or carbon particles or fibers, are added to metallic particles: a further sintering process is applied to the material in order to remove the space holder material and sinter the particles. This type of technique has been largely investigated with titanium particles and various morphologies of carbamide as space holder materials [14–17]. The titanium particles are mixed with the carbamide particles, pressed and subjected to cold isostatic pressing. The space holder is removed with hot water and the remaining green skeleton is sintered at 1200 °C under Ar atmosphere. The typical relative densities are between 0.25 and 0.6, with pore sizes ranging from 150 µm to a few millimeters. Other metals have been used such as stainless steels, superalloys, and even aluminum alloys [18,19].

Concerning the casting route the older way for producing metal foams, for example, was to use infiltration of salt preform by aluminum alloy: the first patent dates to 1962 [20]. The principle is to first obtain a preform of salt (either by sintering or compaction of the salt) and infiltrate this preform at low pressure by pure aluminum or an aluminum alloy [21]. The composite salt/aluminum is then machined to the desired shape and the salt is dissolved in water. The size of the salt particles can be sieved in order to produce foams with regular cell sizes ranging from few 20 µm up to 1 mm. The relative densities of such foams lie between 0.1 and 0.4. The angular shape of the salt can be changed into spherical, leading to

spherical-cell aluminum foams [22,23]. The salt dissolution can be quite long for very fine salt particles. A more recent development of this technique involves the use of a mixture of NaCl, flour and water to produce a large and complex shape for the space holder, which can be infiltrated in the same way as traditional salt preform. The dissolution is much faster and it allows producing aluminum foams with large pore sizes, marketed under the commercial name Corevo [24].

Another way to produce metal foam using a casting technology is to create a preform with compacted sand and a binder. After that, a conventional sand casting technique can be used to infiltrate the preform [25]. The preform is removed in order to produce various kinds of products, including foam parts and dense parts. Various constitutive materials can be used (aluminum alloys, copper alloys, cast iron…) and this is licensed under the name castFoam and designed by Alveotec [26]. It allows producing open-cell foams with cell sizes ranging from 10 mm up to several centimeters, and with a large volume structure.

2.4. Positive replication

In two-step replication techniques, the resulting foam is not the "negative replicate" of the preform, but its "positive replicate": an open-cell polymer sponge is used as the starting material, and a method of investment casting allows the production of metal foam with the same mesostructure. This proceeds as follows [27]: a polyurethane sponge is filled with a slurry of a sufficiently heat-resistant material. This material is dried and the polymer foam is removed by thermal treatment. This enables the mold to rigidify. A ceramic mold of the polymer foam is therefore obtained and is infiltrated with molten metal, possibly under vacuum and/or pressure. After cooling, the mold is removed, by shaking or using pressurized water. Metallic open-cell foam is therefore obtained, which reproduces the initial polymer foam's geometry. This kind of sponge has been manufactured and commercialized by ERG Materials and Corporation (Oakland, CA, USA) under the trade name DuocelTM for many years and display a very regular architecture [28]. Their average cell size ranges from 5 to 100 pores per inch, namely 0.2 µm to 4 mm. Due to their "beam-network-like" shape, they display very low relative density, ranging from 0.03 to 0.12. In theory, a wide range of metals can be used to produce sponges using this technique (e.g., magnesium was used in [29]); however, foams of Al alloys 6101 and A356 are generally produced.

Other techniques allow producing positive replication of polymer foams, but unlike the previous one, the foam will present hollow struts. These techniques are electrodeposition, CVD and CVI. The electrolytic deposition process involves the dissolution of one electrode (the metal) and the deposition of the metal on a second electrode (the polymer template). Because polymer sponges are nonconductive, they must firstly be made electrically conductive by either sputtering or ionic deposition of a thin layer of conductive material. The metal foam is then created by the subsequent electrolytic deposition of the metallic element [30]. Ni and NiCr foams produced by this method are currently manufactured under the trade names Celmet (Sumimoto Electric, Osaka, Japan). The company NiTech® (which has now ceased trading) also produced nickel foams using this route. In this process, a final step of annealing in a reducing atmosphere was performed after removal of the polymer template, in order to lower the amount of oxides that appeared during polymer pyrolysis, which improved the ductility of the resulting foam. These processes are limited to a few metallic elements (alloys are difficult): Ni, NiCr, silver, copper and tin. Relative densities are typically less than 0.1 with average cell sizes from 400 µm up to a few millimeters [31,32].

Pure nickel foams are produced using CVD by Inco limited (Toronto, Ontario, Canada), under the trade name Incofoam®: an open polymer foam is placed in a CVD reactor where nickel tetracarbonyl $NiCO_4$ is introduced. This gas decomposes into Ni and CO at a temperature of about 100 °C and coats all the exposed heated surfaces within the reactor. The polymer is then burnt out in air, and the remaining cellular structure is sintered to densify the ligaments. Chemical Vapor Infiltration (CVI) is also used by Ultramet Advanced Materials and Recemat International to produce refractory metal foams (carbon vitreous, SiC, Ti, Ni, Cu, Al_2O_3) under the trade names Ultrametal and Recemat. Incofoams are produced and traded on a very large scale, probably the largest one as metal foams are concerned. Very low relative density are obtained (between 0.02 and 0.05), and cell sizes between 100 and 300 µm [33–35].

2.5. Foaming from a gas or a precursor

The processing of fully closed cell foams is mainly based, whatever the constitutive material, on gas release in a liquid, a semi-solid or a suspension. Polymer foams are certainly the oldest foams synthesized: their production started with polystyrene foams in the early 1930s and continued with PU foams during and after the World War II. The main processing way is to use a blowing agent at a temperature above the glass temperature of the foam. The use of blowing agents that contribute to ozone layer depletion led to the development of new compounds of this kind. In the gas-blowing technique, the polymer is saturated with a gas or supercritical fluid (usually CO_2 or N_2) at constant temperature and pressure. Then, the system is brought to the supersaturated state either by reducing pressure (pressure induced phase separation) or by increasing temperature (temperature-induced phase separation), resulting in the nucleation and growth of pores [36–39]. The main current polymer foams are PE, PU, PVC, PP and EPS foams, with cell sizes ranging from a few tens of microns up to few millimeters and with relative density ranging from 0.01 up to 0.2 for most of them. Usually there are three main foam categories: flexible foams, rigid foams, and structural foams. And the polymer foams can be open- or closed-cell foams. Among the polymer foams, EPS foams are produced in a different way, using small beads as the starting material. These small beads contain a small percentage of the naturally occurring gas pentane. This gas is impregnated throughout the body

of each small bead. The pre-expansion phase of manufacturing is simply the swelling of the small bead to almost 50 times its original size through heating and rapid release of the gas from the bead during its glass-transition phase.

Concerning the ceramic foams, the gas release is carried out in a ceramic suspension, the following step being a sintering process in order to consolidate the structure [40]. The tricky point is the stabilization of the foam to avoid bubble coalescence, which can be controlled by using a specific surfactant or even particles [41]. The ceramic particles can also be mixed into organic solutions containing the precursors of a polyurethane foam or in molten sucrose [42]. Other techniques using pre-ceramic silicon-based polymers and polyurethane precursors allow obtaining fully closed cell ceramic foams with dense struts. Cell size ranges from 10 μm to 1 mm (lower sizes are obtained when particles are used to stabilize the foam) and porosity up to 95% can be obtained using these techniques [41].

Concerning the metallic foams, two main methods are used: foaming from a gas and foaming from a precursor. As explained in details [43], the oldest mention of metal foams concerns foaming from a gas, and it dates to 1925 [44]. It was then followed by three patents: one on the use of a blowing agent [45], one on foaming from a precursor [46], and one on external gas blowing [47]. Despite these early patents, the major research activity on these materials started in the 1990s. In both cases, the foams had to be stabilized, because the high surface tension and low viscosity of molten metals caused rapid drainage of the liquid towards the bottom of the container and rapid collapse of cell walls, especially at low densities. Stabilization was generally achieved by means of solid additions to the melt, generally in the form of ceramic particles, and also by means of certain alloying elements to the melt.

The *melt foaming process* was developed simultaneously and independently by Alcan [48] and Norsk Hydro [49] in the late 1980s. Both patents are now exploited by the Cymat Aluminum Corporation, Canada [50]. Stabilizing particles, usually SiC or Al_2O_3, are added to the molten aluminum alloy. Gas bubbles are dispersed in the melt using nozzles integrated into a rotor impeller. The bubbles accumulate on the surface of the melt to constitute a foam that is transferred onto a conveyor belt, where it solidifies and cools down. These materials are somewhat anisotropic for two reasons: (i) the foam is passed through the belts, which causes the cells to be oriented; (ii) some gravity drainage occurs during solidification, which leads to a density gradient through the height of the sheet. This process is also used for the manufacture of 3D cast elements: molten aluminum is injected at low pressure: this pressure is sufficient to fill the mold precisely, but it is not so high that it would collapse the cell structure. The cell size is generally between 2.5 to 30 mm with relative densities between 0.02 and 0.2 and restricted to aluminum alloys mainly.

Blowing agent in a liquid. Using a blowing agent in a liquid is an alternative way of creating gas bubbles in a molten metal to cause their nucleation and growth directly within the melt using a gas-producing chemical reaction. One method is to create the bubbles by using a foaming agent that releases gas when heated. This kind of process was developed by the Shinko Wire Company (Amagasaki, Japan), which patented the process in 1987 [51]. The resulting foams were commercialized for industrial applications under the trade name Alporas®. In a first step, 1.5% of Ca is added to the melt in order to increase its viscosity (fine particles of CaO and $CaAl_2O_4$ form due to high affinity of calcium with oxygen). The thickened aluminum is then poured into a casting mold and vigorously stirred with 1.6% TiH_2. As soon as H_2 bubbles are formed and dispersed, the stirring system is withdrawn. The molten material expands and fills the mold. Solidification is obtained by air cooling in the mold. Resulting foam blocks of about 160 kg, with dimensions of $45 \times 202 \times 65$ cm^3) were produced. The cell size is generally between 0.5 and 5 mm, with relative densities between 0.07 and 0.2, and is mainly used with aluminum or magnesium alloys. Other blowing agents like $CaCO_3$ have been investigated by Alcoa [52], which produces such foams.

Blowing agent in solid precursor released in liquid state. The powder mixtures are densified in the solid state using standard techniques: uniaxial or isostatic compression, rod extrusion or powder rolling. Aluminum and its alloys, tin, zinc, brass, lead, gold and some other metals and alloys can be foamed by choosing appropriate blowing agents (TiH_2, $CaCO_3$, ZrH_2 ...) and process parameters. This technique also allows the production of sandwich panels consisting of a metal core and two metal face sheets [53]. These can be made by roll-cladding sheets of metal (aluminum, steel, or titanium) onto a sheet of foamable precursor. Under heat treatment, the core expands, whereas the sheets remain dense. It has been extensively used with pure aluminum and various kind of aluminum alloys [43]. The cell size is generally between 2–10 mm, with a relative density of 0.3 to 0.7.

Blowing agent in solid precursor released in the semi-solid state. In this method, two steps are required to prepare the precursor: (1) the powder blend is predensified in the solid state by cold isostatic pressing, (2) the resulting material is heated to a temperature at which the alloy is semi-solid and can be cast. The final precursor is foamed as described before. One advantage of this process is that the precursor can have a complex shape, and is more isotropic than in the first method. This leads to more homogeneous foams [54]. Note that the advantage in processes using powder compacts and thixocast precursors is that the stabilization is ensured by the presence of oxide skins, so that stabilizing particles are not needed. The cell size is generally between 1 and 5 mm with relative densities of 0.1–0.5. A slightly different method has been also developed: instead of preparing the precursor using metal powders, blowing agent powders (TiH_2) and SiC particles are mixed directly with melts, after which the melt is solidified. This process is known as FORMGRIP, which is an acronym of Foaming of Reinforced Metals by Gas Release in Precursors [55]. The particularity of this method is that TiH_2 particles are firstly heated in the air. This creates an oxide layer TiO_2 on their surface, which avoids premature hydrogen evolution during mixing. This precursor is then reheated in mold in order to produce a foam with very good homogeneity. Note that in this case the constitutive material of the resulting foams is a metal matrix composite. The cell size is generally between 1 and 5 mm, with a relative density of 0.1–0.5.

Blowing agent in powder and resin: it combines foaming and powder metallurgy and proceeds in four steps:

- powder mixing: the constitutive material (e.g., Ni powders), a foaming agent (TSH) and a bonding resin are homogeneously mixed;
- foaming at 150 °C; the heating causes: (i) the resin to melt, (ii) the foaming agent to release gas; this creates bubbles, which are composed of molten resin mixed with Ni solid particles, (iii) the resin is cross-linked. At this step, the resulting foam is made of resin and Ni particles, and it is partially open (some cells communicate);
- thermal decomposition of the resin: small voids are created at the surface of the large bubbles, which leads to a totally open porosity. At this stage, the particles are only bonded by a thin oxide layer of NiO;
- sintering under reducing atmosphere: walls consolidate and the oxide layer disappears. The resulting foam presents large cells containing small cells at their surface and presents a double porosity: (i) a micrometric porosity within the cell walls ($<$10 μm), (ii) a mesometric porosity (about 1 mm) between the cell walls. This double porosity leads to very large specific surfaces (the powder size being around 10 μm), which is an advantage for some properties, such as the permeability. Lastly, materials such as Ti or steel are good candidates for that process. The typical relative densities are between 0.1 and 0.4 [56].

A full list of companies producing metal foams can be obtained on the website dedicated to metal foams [57]; a complete review can be obtained in [58] and in [27,43].

2.6. Additive manufacturing

Additive manufacturing processes have been used for almost 25 years, e.g., Stereo Lithography (SL), Fused Deposition Modeling (FDM), 3D printing, and Laminated Object Manufacturing (LOM). These processes were mainly used for Rapid Prototyping (RP), the prototypes being made from polymer, wood or paper. Important developments have been made recently in the framework of additive manufacturing: new processing routes have emerged, especially the powder bed techniques (e.g., Electron Beam Melting—EBM, Laser Beam Melting—LBM, Selective Laser Sintering—SLS)) and Direct Deposition technologies (e.g., Electron Beam Fabrication FreeForm—EBF^3, Direct Laser Fabrication—DLF, Direct Metal Deposition—DMD, Wire Arc Additive Manufacturing—WAAM) [59–62]. It is now possible to directly manufacture parts that fulfill the engineering specifications in terms of geometry, microstructure, and mechanical behavior. The so-called Rapid Prototyping is now turning into Rapid Manufacturing. These processes definitely open new ways for manufacturing foams or cellular structures with well-controlled geometry and porosity [63–68]. In the following sections, we will give a brief overview of the main additive manufacturing processes and we will highlight their respective advantages and disadvantages. The readers are encouraged to look at [59–61,69,37] among other for more details about the different additive manufacturing processes.

Stereo lithography. In this method, a controlled laser is used to cure a photopolymer resin to shape the component from a 3D CAD model. First, a movable build table (in the Z direction) is set right under the surface of a vat filled with a photosensitive resin of the required material. The property of such a resin is that it gets hard from liquid to solid under exposure to a given wavelength. Usually, stereo lithography process requires ultraviolet rays, but visible light can also be used with some materials. The laser beam then scans and hardens the material through the cross-section of the component by moving in the X–Y plane. Once the layer is cured, the table lowers at a distance of the defined layer thickness and the process is repeated until the final part is built. Highly detailed components and fast delivery are some benefits from the stereo lithography process. The possibility of processing large parts is another notable advantage of this method. On the contrary, manipulating liquid materials (polymers in solution) is messy and this was clearly considered as a disadvantage. In addition, the parts normally require a post-processing treatment in order to make sure that curing is complete. Finally, in many cases, the products do not necessarily show the physical, thermal or mechanical properties typically required from end-user material. The stereo lithography process uses a wide range of photo-sensitive resins that consist of material such as ABS-like materials, polycarbonate, polyethylene, polypropylene.

3D Printing. The 3D printing process uses a cylinder as a material support and a cylinder as a building chamber. For each layer, a roller will spread and compress a measured amount of material powder over the building table. Instead of the laser in the SLS technique, a multichannel jetting head will deposit a liquid adhesive so as to bond the particles of powder and shape the 2D cross section of the component for that layer. Once a layer is completed, the building chamber goes down by an increment of the defined layer thickness, getting ready for the subsequent layer to be printed. After completion of the whole process, the final object will be removed and the excess of powder brushed away. In this method, the use of supports is not necessary, as the powder bed can hold the overhangs. The advantages of 3D are its building rate and low material cost, as well as its relative ease to manufacture color parts. On the other side, its limitation is the resolution, the available materials and the brittleness of the parts produced.

Powder-bed technologies. Most of the additive manufacturing processes rely on a layer-by-layer fabrication that consists of a stack of 2D sections to build the volume, typically the layer thickness is about 20–150 μm. Once building is achieved, the powders that were not bound are removed so as to be recycled and used again in a following building, the part being extracted from the powder bed. Usually, the process can be divided into three steps: (1) the first layer is formed by raking the powders; (2) the powder bed is locally and selectively consolidated in order to manufacture a section of the part—bonding between particles can be achieved using a binder brought by a nozzle or by partial or total melting of the

powders—; (3) once the layer n is built, then the part is lowered by an increment of thickness and the process is repeated to achieve the layer $n+1$ and further until achieving the desired part. The famous processes of Selective Laser Sintering (SLS), Laser Beam Melting (LBM) and Electron Beam Melting (EBM) are based on this principle [70–73,63–67]. The main advantages of the powder-based technologies can be summarized as follows:

(i) these processes do not require a long preparation time before starting the fabrication;
(ii) the raw materials that were not used in building can be recycled and used again in the following fabrication;
(iii) there is a relatively good dimensional accuracy;
(iv) these processes enable to manufacture overhung surfaces;
(v) these processes enable to produce parts that were previously impossible.

The current main drawbacks of these processes are:

(i) only relatively low build rates are achievable;
(ii) only relatively small parts can be built;
(iii) the components have to be built on a flat base.

One has also to keep in mind, for the powder based techniques, that the powders have to meet specific criteria like the sphericity of the particles and their size distribution. These two criteria can be generally achieved by specific powder production processes such gas atomization or plasma atomization. In the case of metallic materials, various alloys have been produced by additive manufacturing. The most used and studied are Ti-alloys (mainly Ti6Al4V), Co–Cr superalloys, titanium aluminides and Ni-based superalloys (Inconel 625 and 718), steels (H13 tool steel), stainless steels (17-4 PH, 316L), and aluminum casting alloys (Al12Si). Other materials are under development or have been investigated at the scale of the laboratory: copper (GRCop-84), niobium, or amorphous metals.

Deposition technologies. The second process that can be used in additive manufacturing is direct deposition (DD). The FDM process is the most famous example of such processes, because it is under democratization in everyday life, probably due to the availability of low-cost machines. This technique uses a heat source (laser, electron beam, or another resistive heating system) in order to melt and deposit the raw material supplied as powder, wire or pellets [74,75]. The advantages of the direct deposition methods over the powder bed technologies are:

(i) a high-rate deposition capability;
(ii) its usability for repairing parts;
(iii) a relatively wide process window;
(iv) a greater ease of manufacturing functionally graded structures or multimaterials. The main limitation is the difficulty to process overhung surfaces.

A variety of metallic alloys have been produced using the DFL or DMD processes, including Ti-alloys, Ni base superalloys, stainless and tool steels. Several materials are available for the well-known FDM process, including: nylon, ABS, polyethylene, among the most used ones.

3. Structure

Fig. 3 summarizes shortly the various structures that can be obtained with each process in the classification that was defined in the introduction. It is interesting to see that only two processes (non-removable space holder stacking) can produce mixed cells with open and close porosities, while the other structure can be produced by several processes.

Concerning the structural parameters that are mostly used to characterize these structure, the first important one is the relative density:

$$\rho = \frac{\rho^*}{\rho_s}$$

where ρ^* is the density of the cellular material, and ρ_s the density of the constitutive material, i.e., the solid from which the cell walls and struts are made. As it will be shown in the next papers, it is the first-order important parameter in all the mechanical and functional properties. Of course this is not the only one and we will now develop the main parameters that are necessary to fully characterize the various foam structures. An important feature is also foam homogeneity, which is well controlled in most processes, but can be less controlled in foaming techniques. For example, the early closed cells metal foams were subjected to a non-homogeneous distribution and therefore it was necessary to quantify this homogeneity. This is of course related to cell size distribution, but often local density measurements were performed either in 2D or 3D from data acquired using X-ray tomography [76].

For the sake of simplicity, we will now present the structural parameters for each structure (closed cells, fully open cells, partially open cells, and mixed cells) and clarify in some cases the effect of processing. In this paper, we will mainly discuss

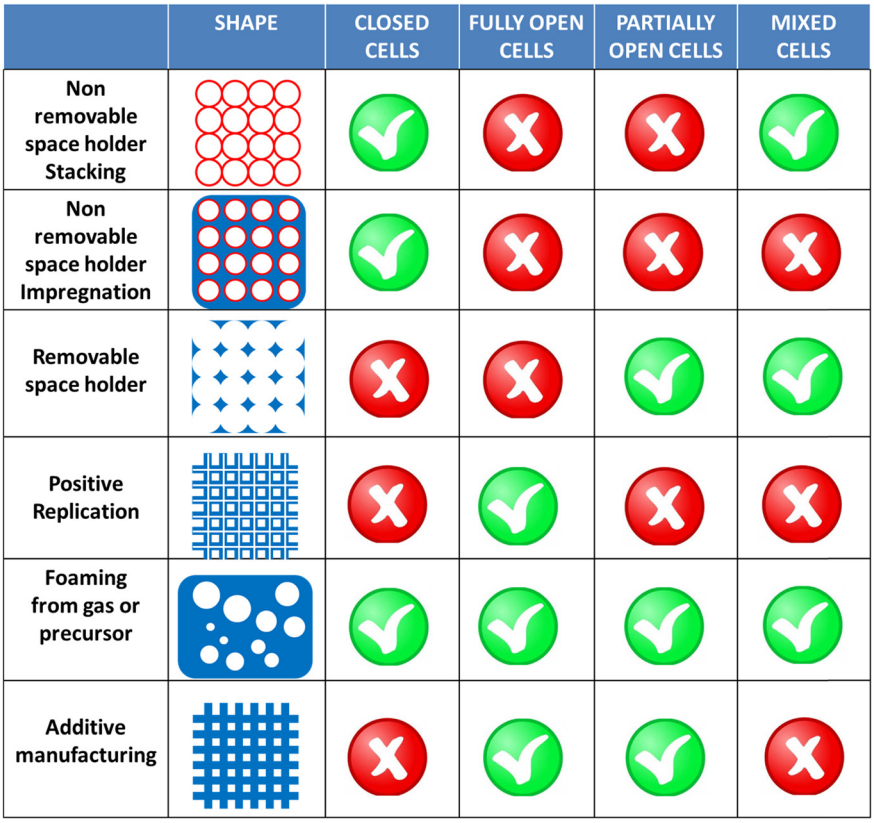

Fig. 3. (Color online.) The possible structure obtained with the main processing techniques.

the structural parameters of the foams and we will not go into the details of the microstructure of the foams, though it has a large impact on some mechanical properties. We will also explain how they can be measured.

3.1. Closed cells

The main important parameters in closed cells are related to the two scales present in these structure, the cells and the struts.

Concerning the cells, the structural parameters are cell morphology, cell size distribution and cell orientation. These parameters are useful to quantify the homogeneity of the foam and therefore the control of the process. The two non-removable space holder techniques present clearly the advantage of fully controlling these parameters, which is of course less the case for the foaming technique, especially for metal foams: indeed, in this case, there was a huge effort concerning the development of controlled structures of the foams. Concerning the struts, the material repartition at the node and along the struts is important as well as the size of the struts. Thanks to X-ray tomography (see the paper dealing with characterization), it is possible to obtain a complete description of the structures using 3D image analysis. When the cell size is roughly spherical, 3D granulometry allows retrieving cell size distribution [77–79]. In the case where the cells are not spherical and one wants to quantify the orientation of the cells, the segmentation of the foam might induce artificial contact between the cells and therefore it often requires more advanced 3D image analysis tools in order to get individual quantifications of each cell [80,79]: this include the separation of the cells using watershed techniques, labeling and structural parameters calculation that can be performed using a 3D quantitative analysis toolbox [81–84], In some metal foams, cracks are present in the faces and thus connectivity indices of the cells can be defined. The strut material distribution and also the ratio of material between the strut and the faces can be obtained from 3D granulometry of the constitutive material [77].

3.2. Fully open cells

In the case of fully open cells, the cell size, cell size distribution is of course important and can be obtained using the same technique as that used for closed cells after cell separation. Other features are often extracted concerning the cells such as the type of polyhedron and the associated parameters (cell volume and strut length distributions, number of faces per cell, number of nodes per face and the shape of the most representative cells) and the way they are joined. This has

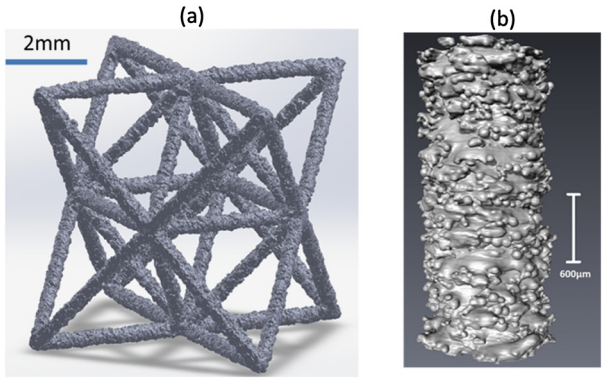

Fig. 4. (a) 3D observation of TA6V structure obtained with EBM; (b) a vertical 1.5-mm-diameter strut. The strut is in its as-built state after manufacturing with EBM. Resolution: 5 µm.

been done in detail for example in Ti foams obtained by electrodeposition techniques. It was concluded that this process leads to the following: the average number of faces per cell is 13, one-third of the cells are dodecahedra, the average number of sides per face is five, 57% of the faces are pentagonal and the most frequent cell in the foam is a dodecahedron with two quadrilaterals, two hexagons and eight pentagons [85]. The morphology of the struts is also particularly important, since it depends on the methods used (positive replication, CVD or CVI). The struts are hollow or not and the section of the struts may be quite different, thus influencing mechanical properties.

Cellular solids (random or periodic) made by any additive manufacturing technique have to be carefully analyzed. The discrepancies between the desired geometry and the produced one should be known. These discrepancies can fluctuate depending on the process, the orientation of the struts, the parameters, the initial raw material… Particular care must be taken in characterizing the geometry, roughness and porosity along the struts. Each of these parameters can affect the thermal, electrical and mechanical properties of the produced cellular structure. For powder-based additive manufacturing, the roughness comes mainly from the powder trapped onto the strut. When producing cellular solids that have strut dimensions ranging in the same scale that the minimal resolution of the process, the control of the final geometry is crucial. Depending on the process, the minimum achievable strut size can range from 100 µm to a few millimeters. Tomographic characterization allows us to assess these properties and to take them into consideration for simulation. The 3D quantification of struts made by LBM [86,87] showed the geometry roughness of the strut and the pore size distribution. Discrepancies in terms of geometry are visible for small strut diameters (∼100 µm), as shown in Fig. 4. When producing small-diameter struts by EBM (∼1 mm), the mechanically efficient volume is reduced as the roughness begins to represent the main part of the strut [67]. This mechanically efficient volume can be used in numerical simulation to compute the ‘true’ properties of the cellular solid. Improvements have to be made for a better control of the geometric accuracy of cellular solids made by additive manufacturing and to minimize its residual porosity. The key parameters for this control are the process parameters and the strategy. Post-treatment can also be carried out to improve the inner roughness of cellular solids created by additive manufacturing (chemical etching or electrochemical polishing).

3.3. Partially open cells

Partially open cells require also the characterization of cell size and distribution using the same techniques as those presented below. Another important parameter is the quantification of the opening degree of these foams. For example, when negative replication with salt is used, the compaction pressure applied to the salt preform allows one to control the neck size between the particles, which results in opening windows between the cells and also the coordination number of the cells. To obtain these two parameters, the cells have to be split using 3D watershed techniques. Generally, the “window size” is related to the relative density, increasing while relative density decreases [88,89,22,23,90,91]. Concerning the cell coordination number, it was shown that it basically followed Artz’s law [92] when compaction is used to densify the salt preform: it decreases linearly with relative density with some deviation to the original law related to the shape of the particle [93]. Coordination numbers have also been measured in polymeric foam from tomography data [94]. As an example, Fig. 5 presents the 3D rendering of various aluminum foams produced with the salt replication technique showing the increase of the opening degree as relative density decreases. The physical and mechanical properties of these foams are highly related to these two main parameters, as it will be shown in the other papers of this dossier. As an example, the permeability of the foam can be directly related to the size of these windows, as shown by [95].

3.4. Mixed cells

Mixed cells present open and close porosities and therefore the main parameters are of course the already mentioned parameters for open and close cells. It is obtained for example from hollow sphere stacking or from foams obtained with

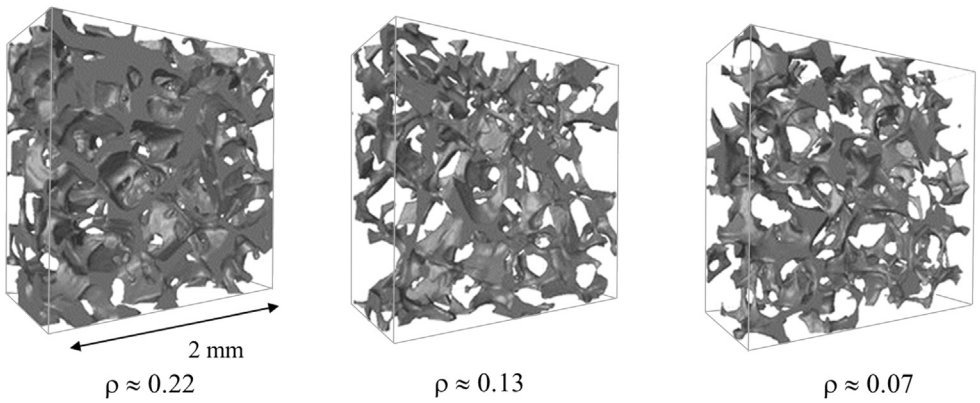

Fig. 5. 3D rendering of pure aluminum foam obtained using the salt replication technique at EPFL with various relative densities [88].

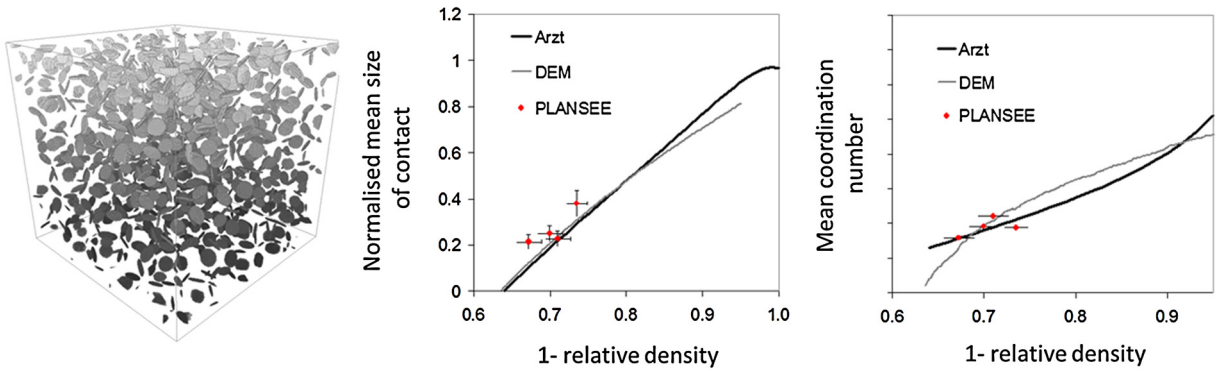

Fig. 6. 3D rendering of the neck between hollow spheres in a random hollow sphere stacking from PLANSEE with the quantification of the normalized mean contact size and the mean coordination number versus relative density: it correlates well with the analytical model of Artz or numerical simulation [99].

the powder technology. Of course one has to quantify the volume fraction of open and close porosity, which is quite easy to obtain thanks to X-ray tomography [96,17]. As for the other structure, the cells wall is an important parameter and can be obtained using the granulometry technique. Another important parameter in the case of hollow sphere stacking is the neck size between the hollow sphere and the coordination number of the cells. This can be obtained after some 3D image analysis treatment, and Fig. 6 presents the mean neck size and coordination number from 3D data, which correlate well with Artz's compaction law or DEM calculation [92,97]: this is explained by the fact that the polystyrene spheres are compacted to create bonds between spheres in the processing. The neck size has a great importance on the mechanical properties of these hollow sphere stackings [98].

4. Conclusion

In this paper, we present the various processes and their main characteristics that allow producing cellular structures with various topologies (open cells, closed cells, partially open cells and mixed cell) and for various constitutive materials such as polymer, ceramic and metals with a specific focus on metals. We also present the main characteristics that are necessary for a complete characterization of these structures and the way to obtain them: the relative density, local density, open-cell volume fraction, closed-cell volume fraction, cell-size distribution, cell-wall distribution, material distribution between cells and struts, roughness of the struts, cell coordination number, contact size between cells. All these characteristics are easily accessible thanks to X-ray tomography and 3D quantitative analysis. It is of importance to mention, in addition to these parameters, that the defects in the constitutive materials (cracks, intermetallics, small pores…) that may be induced by the processing should also be characterized.

References

[1] L.J. Gibson, M.F. Ashby, Cellular Solids—Structure and Properties, second ed., Cambridge University Press, 1997, p. 510.
[2] A. Öchsner, C. Augustin, Multifunctional Metallic Hollow Sphere Structures, Springer, 2009, 251 pages.
[3] http://www.ifam.fraunhofer.de/en/Dresden/Cellular_metallic_materials/Hohlkugelstrukturen.html, last access October 2014.
[4] http://hollomet.com/en/home.html, last access October 2014.
[5] K. Stöbener, D. Lehmhus, N. Zimmer, J. Baumeister, German Patent, DE 103 28 047, 2005 (2005).

[6] J. Baumeister, J. Weise, E. Hirtz, K. Höhne, J. Hohe, Applications of aluminum hybrid foam sandwiches in battery housings for electric vehicle, Proc. Mater. Sci. 4 (2014) 301–305.
[7] http://www.plasticstoday.com/sites/default/files/Web_D_TPO_3M_IM%20Guidelines_glass_bubbles.pdf, last access October 2014.
[8] http://www.envirospheres.com/products.asp, last access October 2014.
[9] http://www.ceminerals.com/scopi/group/ceminerals/ceminerals.nsf/pagesref/LONL-942J2N/$file/KKWBUBBLE.pdf, last access October 2014.
[10] http://www.palmerholland.com/Assets/CE/Documents/data-sheets/S60%20Glass%20Bubbles.pdf, last access October 2014.
[11] B.H. Rutz, J.C. Berg, A review of the feasibility of lightening structural polymeric composites with voids without compromising mechanical properties, Adv. Colloid Interface Sci. 160 (2010) 56–75.
[12] J.A. Santa Maria, B.F. Schultz, J.B. Ferguson, N. Gupta, P.K. Rohatgi, Effect of hollow sphere size and size distribution on the quasi-static and high strain rate compressive properties of Al-A380–Al_2O_3 syntactic foams, J. Mater. Sci. 49 (2014) 1267–1278.
[13] I. Norbet Orbulov, Metal matrix syntactic foams produced by pressure infiltration, the effect of infiltration parameters, Mater. Sci. Eng. A, Struct. Mater.: Prop. Microstruct. Process. (2013) 11–19.
[14] A. Laptev, M. Bram, A.P. Buchkremer, D. Stöver, Study of production route for titanium parts combining very high porosity and complex shape, Powder Metall. 47 (1) (2004) 85–92.
[15] A. Laptev, O. Vyal, M. Bram, H.P. Buchkremer, D. Stöver, Green strength of powder compacts provided for production of highly porous titanium parts, Powder Metall. 48 (4) (2005) 358–364.
[16] C.F. Li, Z.G. Zhu, T. Liu, Powder Metall. 48 (3) (2005) 237–240.
[17] N. Tuncer, E. Maire, L. Salvo, G. Arslan, Investigation of p/m parameters' effect on architecture of titanium foams using X-ray microtomography, Mater. Sci. Eng. A, Struct. Mater.: Prop. Microstruct. Process. 530 (2011) 633–642.
[18] M. Bram, C. Stiller, H.P. Buchkremer, D. Stover, H. Baur, High-porosity titanium, stainless steel and superalloy parts, Adv. Eng. Mater. 2 (2000) 196.
[19] Y.Y. Zhao, D.X. Dun, A novel sintering-dissolution process for manufacturing Al foams, Scr. Mater. 44 (2001) 341.
[20] Cellular materials: new concepts provide unique possibilities—feature article, The Iron Age, February 8 (1962), pp. 119–121.
[21] C. San Marchi, J.F. Despois, A. Mortensen, Uniaxial deformation of open-cell aluminum foam: the role of internal damage, Acta Mater. 49 (2001) 3959.
[22] R. Goodall, A. Marmottant, L. Salvo, A. Mortensen, Spherical pore replicated microcellular aluminium: processing and influence on properties, Mater. Sci. Eng. A, Struct. Mater.: Prop. Microstruct. Process. 465 (2007) 124–135.
[23] R. Goodall, A. Marmottant, L. Salvo, A. Mortensen, Spherical pore replicated microcellular aluminium: processing and influence on properties, Mater. Sci. Eng. A, Struct. Mater.: Prop. Microstruct. Process. 465 (1–2) (2007) 124.
[24] http://www.innovationcells.ch/en/projects/aluminium-foam/just-mix-salt-flour-water-and-aluminium.html, last access October 2014.
[25] J. Dairon, Y. Gaillard, J.-C. Tissier, D. Balloy, G. Degallaix, Parts containing open-celled metal foam manufactured by the foundry route: processes, performances and applications, Adv. Eng. Mater. 13 (2011) 1066–1071.
[26] http://www.alveotec.fr, last access October 2014.
[27] J. Banhart, Manufacture, characterisation and application of cellular metals and metal foams, Prog. Mater. Sci. 46 (2001) 559–632.
[28] http://www.ergaerospace.com/Aluminum-properties.htm, last access October 2014.
[29] Y. Yamada, K. Shimojima, Y. Sakaguchi, M. Mabuchi, M. Nakamura, T. Asahina, T. Mukai, H. Kanahashi, K. Higashi, Processing of an open-cellular AZ91 magnesium alloy with a low density of 0.05 g/cm^3, J. Mater. Sci. Lett. 18 (1999) 1477–1480.
[30] D.T. Queheillalt, D.J. Sypeck, H.N.G. Wadley, Synthesis of open-cell metal foams by templated directed vapor deposition, J. Mater. Res. 16 (2000) 1028–1036.
[31] http://www.dunlop-equipment.com/prod_retimet.htm, last access October 2014.
[32] http://www.nickelfoam.cn/info/Nickel-foam-130-1.htm, last access October 2014.
[33] http://www.novametcorp.com/products/incofoam/, last access October 2014.
[34] http://www.ultramet.com/refractoryopencells.html, last access October 2014.
[35] http://www.recemat.nl/eng, last access October 2014.
[36] S.K. Goel, E.J. Beckman, Generation of microcellular polymeric foams using supercritical carbon dioxide. I. Effect of pressure and temperature on nucleation, Polym. Eng. Sci. 34 (1994) 1137–1147.
[37] K.A. Arora, A.J. Lesser, J.T. McCarthy, Preparation and characterization of microcellular polystyrene foams in supercritical carbon dioxide, Macromolecules 31 (1998) 4614–4620.
[38] E. Reverchon, S. Cardea, Production of controlled polymeric foams by supercritical CO_2, J. Supercrit. Fluids 40 (2007) 144–152.
[39] I. Tsivintzelis, A.G. Angelopoulou, C. Panayiotou, Foaming of polymers with supercritical CO_2: an experimental and theoretical study, Polymer 48 (2007) 5928–5939.
[40] T. Ohji, M. Fukushima, Macro porous ceramics: processing and properties, Int. Mater. Rev. 57 (2012) 115–131.
[41] A.R. Studart, U.T. Gonzenbach, E. Tervoort, Ludwig J. Gauckler, Processing routes to macroporous ceramics: a review, J. Am. Ceram. Soc. 89 (6) (2006) 1771–1789.
[42] S. Vijayan, R. Narasimman, C. Pruvdi, K. Prabhakaran, Preparation of alumina foams by the thermo-foaming of powder dispersions in molten sucrose, J. Eur. Ceram. Soc. 34 (2014) 425–433.
[43] J. Bahnart, Light-metal foams—history of innovation and technological challenges, Adv. Eng. Mater. 15 (3) (2013) 82–111, special issue.
[44] M.A. De Meller, French Patent 615,147, 1926.
[45] J.C. Elliott, Method of producing metal foam, USA Patent 2,751,289, 1956 (1951).
[46] B.C. Alen, Method of making foamed metal, United States Patent No. 3,087,807, filed 4th Dec 1959.
[47] W.S. Fiedler, Method of making metal foam bodies, USA Patent 3,214,265, 1965 (1963).
[48] I. Jin, L.D. Kenny, H. Sang, Method of producing lightweight foamed metal, USA Patent 4,973,358, 1990 (1989).
[49] W.W. Ruch, B. Kirkevag, A process of manufacturing particle reinforced metal foam and product thereof, European Patent 0 483 184, 1994 (1990).
[50] http://www.cymat.com/, last access October 2014.
[51] S. Akiyama, H. Ueno, K. Imagawa, A. Kitahara, S. Nagata, K. Morimoto, T. Nishikawa, M. Itoh, Foamed metal and method of producing same, European Patent 0 210 803, 1989 (1986).
[52] J.D. Bryant, J.A. Kallivayalil, M.D. Crowley, J.R. Genito, L.F. Wieserman, D.M. Wilhelmy, W.E. Boren, Method for producing foamed aluminum products by use of selected carbonate decomposition products, USA Patent 7,452,402, 2008 (2005).
[53] J. Baumeister, J. Banhart, M. Weber, Verfahren zur Herstellung eines metallischen Verbundwerkstoffs [Process for manufacturing metallic composite materials], German Patent 44 26 627, 1994.
[54] H. Stanzick, M. Wichmann, J. Weise, L. Helfen, T. Baumbach, J. Banhart, Adv. Eng. Mater. 4 (2002) 814.
[55] V. Gergely, T.W. Clyne, The effect of oxide layers on gas-generating hydride particles during production of aluminium foams, in: D.S. Schwartz, D.S. Shih, A.G. Evans, H.N.G. Wadley (Eds.), Porous and Cellular Materials for Structure Applications, Materials Research Society, Warrendale, 1998, p. 139.
[56] M. Gauthier, L.P. Lefebvre, Y. Thomas, M.N. Bureau, Production of metallic foams having open porosity using a powder metallurgy approach, Mater. Manuf. Process. 19 (5) (2004) 793–811.
[57] http://www.metalfoam.net/companies.html.

[58] R. Goodall, A. Mortensen, Porous metals, in: David E. Laughlin, Kazuhiro Hono (Eds.), Physical Metallurgy, vol. 24, fifth edition, Elsevier, 2014.
[59] K.V. Wong, A. Hernandez, A review of additive manofacturing, ISRN Mech. Eng. 2012 (2012) 208760, pp. 10.
[60] W.E. Frazier, Metal additive manufacturing: a review, J. Mater. Eng. Perform. (2014) 1917–1928.
[61] B. Vayre, F. Vignat, F. Villeneuve, Metallic additive manufacturing: state-of-the-art review and prospects, Mech. Ind. 13 (2012) 89–96.
[62] L.E. Murr, S.M. Gaytan, D.A. Ramirez, E. Martinez, J. Hernandez, K.N. Amato, P.W. Shindo, F.R. Medina, R.B. Wicker, Metal fabrication by additive manufacturing using laser and electron beam melting technologies, J. Mater. Sci. Technol. 28 (2012) 1–14.
[63] L.E. Murr, S.M. Gaytan, F. Medina, H. Loez, E. Martinez, B.I. Machado, D.H. Hernandez, L. Martinez, M.I. Lopez, R.B. Wicker, J. Bracke, Next-generation biomedical implants using additive manufacturing of complex cellular and functional mesh arrays, Philos. Trans. R. Soc. A 368 (2010) 1999–2032.
[64] L.E. Murr, K.N. Amato, S.J. Li, Y.X. Tian, X.Y. Cheng, S.M. Gaytan, E. Martinez, P.W. Shindo, F. Medina, R.B. Wicker, Microstructure and mechanical properties of open cellular biomaterials prototypes for total knee replacement implants fabricated by electron beam melting, J. Mech. Behav. Biomed. Mater. 4 (2011) 1396–1411.
[65] P. Heinl, L. Muller, C. Korner, R.F. Singer, F.A. Muller, Cellular Ti–6Al–4V structures with interconnected macro porosity for bone implants fabricated by selective electron beam melting, Acta Biomater. 4 (2008) 1538–1544.
[66] E. Marin, S. Fusi, M. Pressaco, L. Paussa, Characterization of cellular solids in Ti6Al4V for orthopaedic implant applications: trabecular titanium, J. Mech. Behav. Biomed. Mater. 3 (2010) 373–381.
[67] M. Suard, P. Lhuissier, R. Dendievel, J.J. Blandin, F. Vignat, F. Villeneuve, Towards stiffness prediction of cellular structures made by electron beam melting (EBM), Powder Metall. 57 (3) (2014) 190–195.
[68] M. Aliakbari, Additive manufacturing: state-of-the-art, capabilities, and sample applications with cost analysis, Master thesis, Department of Industrial Production, KTH University, 2012.
[69] A.A. Antonysamy, Microstructure texture and mechanical property evolution during additive manufacturing of Ti6Al4V alloy for aerospace applications, Thesis, Department of Materials Engineering, University of Manchester, 2012.
[70] T. Vilaro, C. Colin, J.D. Bartout, As fabricated and heat-treated microstructures of the Ti6Al4V alloy processed by selective laser melting, Metall. Mater. Trans. A, Phys. Metall. Mater. Sci. 39A (2008) 3190–3199.
[71] P.A. Kobryn, S. Semiatin, The laser additive manufacturing of Ti–6Al–4V, JOM 53 (2011) 40–43.
[72] K. Kempen, L. Thijs, J. Van Humbeeck, J.-P. Kruth, Mechanical properties of AlSi10Mg produced by selective laser melting, Phys. Proc. 39 (2012) 439–446.
[73] B. Ahuja, M. Karg, K.Y. Nagulin, M. Schmidt, Fabrication and characterization of high strength Al-Cu alloys processed using laser beam melting in metal powder bed, Phys. Proc. 56 (2014) 135–146.
[74] W. Fude, J. Mei, X. Wu, Microstructure study of direct laser fabricated Ti alloys using powder and wire, Appl. Surf. Sci. 253 (2006) 1424–1430.
[75] E. Brandl, V. Michailov, B. Viehweger, C. Leyens, Deposition of Ti6Al4V using laser and wire. Part I. Microstructural properties of single beads, Surf. Coat. Technol. 206 (2011) 1120–1129.
[76] H.P. Degischer, A. Kottar, On the non-destructive testing of metal foams, in: J. Banhart, F. Ashby, N.A. Fleck (Eds.), Metal Foams and Porous Metal Structures, Verlag MIT Publishing, 1999, pp. 213–220.
[77] A. Elmoutaouakkil, L. Salvo, E. Maire, G. Peix, 2D and 3D characterisation of metal foams using X ray tomography, Adv. Eng. Mater. 4 (10) (2002) 803.
[78] O.B. Olurin, M. Arnold, C. Körner, R.F. Singer, The investigation of morphometric parameters of aluminium foams using micro-computed tomography, Mater. Sci. Eng. A 328 (2002) 334–343.
[79] O. Brunke, S. Odenbach, F. Beckmann, Structural characterization of aluminium foams by means of microcomputed tomography, in: Optical Science and Technology, the SPIE 49th Annual Meeting International Society for Optics and Photonics, 2004, pp. 453–463.
[80] A.H. Benouali, L. Froyen, T. Dillard, S. Forest, F. N'guyen, Investigation on the influence of cell shape anisotropy on the mechanical performance of closed cell aluminium foams using micro-computed tomography, J. Mater. Sci. 40 (22) (2005) 5801–5811.
[81] J. Vicente, F. Topin, J.V. Daurelle, Open celled material structural properties measurement: from morphology to transport properties, Mater. Trans. 47 (9) (2006) 2195–2202.
[82] K. Mader, R. Mokso, C. Raufaste, B. Dollet, S. Santucci, J. Lambert, M. Stampanoni, Quantitative 3D characterization of cellular materials: segmentation and morphology of foam, Colloids Surf. A, Physicochem. Eng. Asp. 415 (2012) 230–238.
[83] http://imorph.sourceforge.net/.
[84] http://simap.grenoble-inp.fr/le-laboratoire/m-luc-salvo–430404.kjsp?RH=SIMAP_ANNUAIRE2.
[85] T. Dillard, F. Nguyen, E. Maire, S. Forest, Y. Bienvenu, J.-D. Bartout, M. Croset, L. Salvo, R. Dendievel, P. Cloetens, 3D quantitative image analysis of open-cell nickel foams under tension and compression loading using X-ray microtomography, Philos. Mag. 85 (2005) 2147.
[86] T.B. Kim, S. Yue, Z. Zhang, E. Jones, J.R. Jones, P.D. Lee, Additive manufactured porous titanium structures: through-process quantification of pore and strut networks, J. Mater. Process. Technol. 214 (11) (2014) 2706–2715.
[87] G. Pyka, A. Burakowski, G. Kerckhofs, M. Moesen, S. Van Bael, J. Schrooten, M. Wevers, Surface modification of Ti6Al4V open porous structures produced by additive manufacturing, Adv. Eng. Mater. 14 (6) (2012) 363–370.
[88] PhD INPG, 2006.
[89] R. Goodall, J.F. Despois, A. Marmottant, L. Salvo, A. Mortensen, The effect of preform processing on replicated aluminium foam structure and mechanical properties, Scr. Mater. 54 (12) (2006) 2069.
[90] E. Maire, P. Colombo, J. Adrien, L. Babout, L. Biasetto, Characterization of the morphology of cellular ceramics by 3D image processing of X-ray tomography, J. Eur. Ceram. Soc. 27 (2007) 1973–1981.
[91] L. Salvo, M. Suéry, A. Marmottant, N. Limodin, D. Bernard, 3D Imaging in material science: application of X-ray tomography, C. R. Phys. 11 (2010) 641–649.
[92] E. Arzt, The influence of an increasing particle coordination on the densification of spherical powders, Acta Metall. 30 (1982) 1883–1890.
[93] A. Marmottant, L. Salvo, C.L. Martin, A. Mortensen, Coordination measurements in compacted NaCl irregular powders using X-ray microtomography, J. Eur. Ceram. Soc. 28 (2008) 2441–2449.
[94] B.M. Patterson, K. Henderson, Z. Smith, Measure of morphological and performance properties in polymeric silicone foams by X-ray tomography, J. Mater. Sci. 48 (2013) 1986–1996.
[95] J.F. Despois, A. Mortensen, Permeability of open-pore microcellular materials, Acta Mater. 53 (2005) 1381–1388.
[96] PhD INPG, 2009.
[97] C.L. Martin, D. Bouvard, S. Shima, Study of particle rearrangement during powder compaction by the discrete element method, J. Mech. Phys. Solids 51 (2003) 667–693.
[98] A. Fallet, P. Lhuissier, L. Salvo, C.L. Martin, A. Wiegmann, M. Kabel, Multifunctional optimization of random hollow sphere stackings, Scr. Mater. 68 (1) (2013) 35–38.
[99] A. Fallet, P. Lhuissier, L. Salvo, Y. Bréchet, Mechanical behaviour of metallic hollow spheres foam, Adv. Eng. Mater. 10 (9) (September 2008) 858.